JACS
JOURNAL OF THE AMERICAN CHEMICAL SOCIETY

Article

pubs.acs.org/JACS

Decoupled Associative and Dissociative Processes in Strong yet Highly Dynamic Host–Guest Complexes

Eric A. Appel,[*,†,⊥] Frank Biedermann,[*,‡,⊥] Dominique Hoogland,[¶] Jesús del Barrio,[§] Max D. Driscoll,[∥] Sam Hay,[∥] David J. Wales,[¶] and Oren A. Scherman[*,¶]

[†]Department of Materials Science and Engineering, Stanford University, Stanford California 94305, United States

[‡]Institute of Nanotechnology, Karlsruhe Institute of Technology (KIT), Hermann-von-Helmholtz Platz 1, 76344 Eggenstein-Leopoldshafen, Germany

[¶]Department of Chemistry, University of Cambridge, Lensfield Road, Cambridge CB2 1EW, U.K.

[§]Schlumberger Gould Research Center, High Cross, Madingley Road, Cambridge CB3 0EL, U.K.

[∥]Manchester Institute of Biotechnology and School of Chemistry, University of Manchester, 131 Princess Street, Manchester M1 7DN, U.K.

[⊥]Department of Chemistry, University of Cambridge, Lensfield Road, Cambridge CB2 1EW, U.K.

Supporting Information

ABSTRACT: Kinetics and thermodynamics in supramolecular systems are intimately linked, yet both are independently important for application in sensing assays and stimuli-responsive switching/self-healing of materials. Host–guest interactions are of particular interest in many water-based materials, sensing, and drug delivery applications. Herein we investigate the binding dynamics of a variety of electron-rich aromatic moieties forming hetero-ternary complexes with the macrocycle cucurbit[8]uril (CB[8]) and an auxiliary guest, dimethyl viologen, with high selectivity and equilibrium binding constants (K_{eq} up to 10^{14} M^{-2}). Using stopped-flow spectrofluorimetry, association rate constants were observed to approach the diffusion limit and were found to be insensitive to the structure of the guest. Conversely, the dissociation rate constants of the ternary complexes varied dramatically with the guest structure and were correlated with the thermodynamic binding selectivity. Hence differing molecular features were found to contribute to the associative and dissociative processes, mimicking naturally occurring reactions and giving rise to a decoupling of these kinetic parameters. Moreover, we demonstrate the ability to exploit these phenomena and selectively perturb the associative process with external stimuli (e.g., viscosity and pressure). Significantly, these complexes exhibit increased binding equilibria with increasing pressure, with important implications for the application of the CB[8] ternary complex for the formation of hydrogels, as these gels exhibit unprecedented pressure-insensitive rheological properties. A high degree of flexibility therefore exists in the design of host–guest systems with tunable kinetic and thermodynamic parameters for tailor-made applications across a broad range of fields.

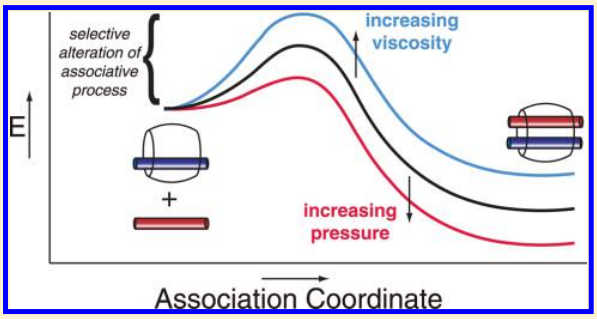

INTRODUCTION

High association and dissociation rates are often desirable for applications relying on fast molecular recognition events such as for sensing assays and stimuli-responsive switching/self-healing systems.[1−3] Materials utilizing supramolecular moieties that rely on slowly exchanging metal–ligand bonds or non-covalent interactions requiring significant conformational rearrangement for association/dissociation have indeed demonstrated self-healing, yet only at high temperatures where exchange kinetics are reasonably rapid.[4,5] Moreover, the kinetics of association and dissociation play a crucial role in determining the bulk properties of supramolecular cross-linked materials,[6−9] as well as the utility of inhibitors in pharmaceutical practice.[10,11] These kinetics features, however, are unknown for the vast majority of supramolecular moieties that are being utilized in an ever broadening spectrum of applications. Furthermore, scant research has been published detailing supramolecular moieties that provide the opportunity to selectively tune the kinetic and thermodynamic features for a particular application.

The macrocyclic host family of cucurbit[n]uril (CB[n]; n = 5, 6, 7, 8, and 10; Figure 1a), is widely used for self-assembly and sensing applications in aqueous solution.[1,12−15] A unique feature of the CB[n] hosts is their exceptionally strong affinity for a wide range of guests in aqueous solutions.[16,17] Cucurbit[8]uril (CB[8]) has a large cavity volume (ca. 360 Å^3)[16,17] and can simultaneously accommodate two

Received: May 10, 2017
Published: June 29, 2017

DOI: 10.1021/jacs.7b04821
J. Am. Chem. Soc. 2017, 139, 12985−12993

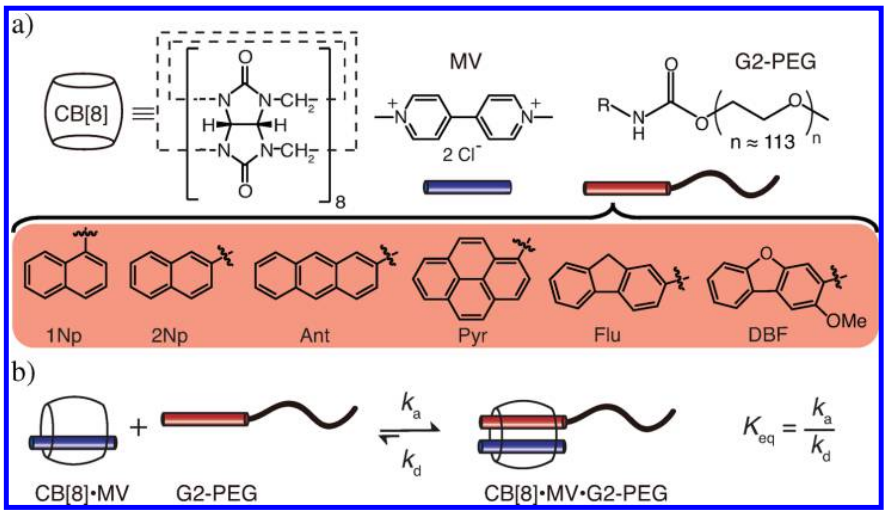

Figure 1. (a) Chemical structures of the macrocyclic host cucurbit[8]uril (CB[8]), the auxiliary first guest dimethyl viologen (MV), and the second-guest-labeled poly(ethylene glycol) (G2-PEG). (b) Schematic representation of the ternary complex formation and definition of the corresponding rate constants.

Table 1. Tabulated Kinetic and Thermodynamic Data for CB[8]·MV·G2-PEG Ternary Complex Formation in Water

guest	k_a[a] (10^7; M^{-1} s^{-1})	k_d[a] (s^{-1})	$K_{eq}(2)$[a,b] (10^4; M^{-1})	$K_{eq}(2)$[c] (10^4; M^{-1})	$K_{eq}(2)$[d] (10^4; M^{-1})	$K_{eq}(2)$[e] (10^4; M^{-1})
1 Np-PEG	2.5 ± 0.3	390 ± 40	4 ± 1	n.a.	3 ± 1	1.4 ± 0.5
2Np-PEG	4 ± 2	≤200	≥20	n.a.	14 ± 4	7.8 ± 1.5
Ant-PEG	2.8 ± 0.1	≤10	≥280	200 ± 150	44 ± 10	n.a.
Flu-PEG	2.8 ± 0.1	≤10	≥280	5 ± 2	5 ± 1	4.3 ± 1.0
DBF-PEG	2.2 ± 0.1	32 ± 6	68 ± 15	22 ± 10	13 ± 4	11 ± 2
Pyr-PEG	1.9 ± 0.1	8 ± 3	230 ± 90	22 ± 10	13 ± 4	11 ± 2

[a]Values reported for 5 °C. [b]Equilibrium binding constants calculated *via* $K_{eq}(2) = k_a/k_d$. [c]From extrapolation of stopped flow kinetic data to 25 °C with [G2-PEG] = 1 μM. [d]From static fluorescence titration experiments at 25 °C with [G2-PEG] = 2 μM. [e]From ITC experiments at 25 °C with [G2-PEG] = 1 mM.

guests (Figure 1b).[12−14,18,19] The formation of ternary complexes with CB[8] occurs in a stepwise binding process whereby an electron-deficient guest, such as viologen (MV), enters the CB[8] cavity first, forming a self-assembled receptor for a range of electron-rich second-guests with a $K_{eq} > 10^6$ M^{-1} (Figures 1 and S4).[18,20,21] Most neutral aromatic second-guests bind with $K_{eq}(2)$ in the range of 10^2−10^6 M^{-1}, where a combination of electrostatic and solvation effects largely determines the second-guest selectivity.[22,23] As a result of the high binding constants and well-defined ternary complex composition, CB[8] ternary complex formation has been utilized in a number of applications, ranging from the assembly of molecular necklaces,[20] sequence selective recognition of peptides,[24−26] surface modifications,[26−29] and protein conjugations[30−32] to the formation of nanocapsules,[33] nanocomposites,[34] nanoparticles,[35] and hydrogels.[8,36−40]

Despite the growing interest in CB[8] chemistry, the kinetic features of the ternary complex formation, while being indispensable to their applicability, have been unknown. Herein we investigate the association and dissociation rates of a series of second guests binding to a self-assembled receptor of first guest and CB[8] (CB[8]·MV) and demonstrate that differing molecular features direct these processes. Moreover, we show that this property can be exploited to elicit independent control over the kinetic processes within the CB[8] ternary binding equilibrium, imparting a high degree of tunability in both the kinetic and thermodynamic parameters of these host−guest systems.

RESULTS

Kinetics of CB[8] Ternary Complex Formation. The fluorescence quenching of an emissive second guest upon binding to CB[8]·MV is well suited to study the ternary complex formation in dilute aqueous solutions,[18,23,24,41] as it allows for the real-time monitoring of ternary complex formation after rapid mixing.[42] Additionally, undesirable self-aggregation of the hydrophobic second guests can be avoided at low concentrations (2 μM). Thus, fluorescent second guests such as naphthalene (Np), anthracene (Ant), pyrene (Pyr), fluorene (Flu), and dibenzofuran (DBF) were selected for this study (Figure 1a). These second-guest moieties were conjugated to the hydroxyl end-group of poly(ethylene glycol)-monomethyl ether chains (M_n = 5000 g/mol)[43] to ensure sufficient solubility in aqueous solutions and to reduce the apparent rate of ternary complex formation to such an extent that it can be measured by stopped-flow experiments, which exhibit a mixing dead-time of approximately 1 ms. Prior to stopped-flow experiments, ternary complex formation of G2-PEG and CB[8]·MV was confirmed by fluorescence titration and isothermal titration calorimetry (ITC) experiments, and the $K_{eq}(2)$ values obtained for second-guest binding from these two measurements are in good agreement (Table 1;

DOI: 10.1021/jacs.7b04821
J. Am. Chem. Soc. 2017, 139, 12985−12993

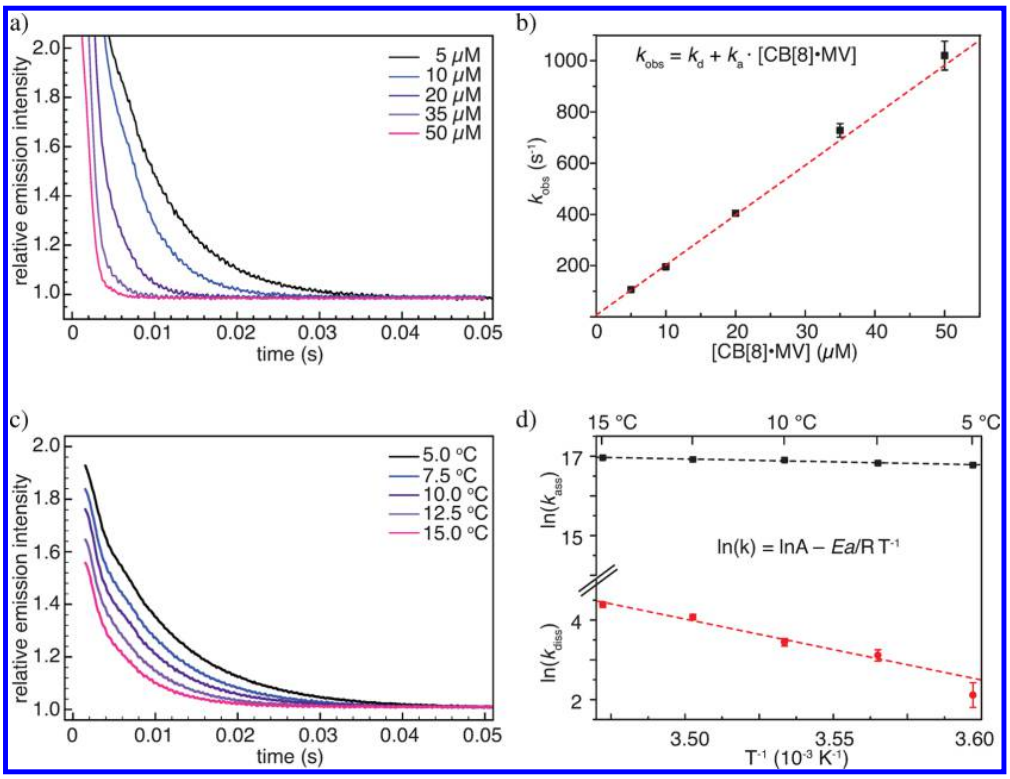

Figure 2. Characterization of kinetic parameters in CB[8] binding. (a) Kinetic traces measured by stopped flow experiments at 5 °C with variation of the concentration of CB[8]·MV (5–50 μM) in the reaction cell while keeping the concentration of Pyr-PEG (1 μM) constant. (b) Plot of k_{obs} against the concentration of CB[8]·MV and the best linear fit to extract k_a and k_d. (c) Kinetic traces measured by stopped flow experiments at various temperatures with a concentration of Pyr-PEG (1 μM) and CB[8]·MV (5 μM) in the reaction cell. (d) Arrhenius plot of ln(k_a) and ln(k_d) vs T^{-1} and the best linear fits to determine Ea_a and Ea_d, respectively.

fluorescence data are shown in Figures S2 and S3, while ITC data are shown in Figure S5).

In stopped-flow experiments the quenching of the G2-PEG fluorescence emission is recorded after rapid mixing of G2-PEG and CB[8]·MV solutions. Monoexponential fits of the fluorescence intensity decay according to $I = I_0 + I_\infty\ e^{-k_{obs}t}$ yielded the observed rate constants (k_{obs}) as a function of $[CB[8]\cdot MV]_0$ (see Figure 2a for the example of Pyr-PEG). In the pseudo-first-order approximation, i.e., $[CB[8]\cdot MV]_0 \gg [G2\text{-}PEG]_0$, the individual rate constants k_a and k_d can be obtained from $k_{obs} = k_a[CB[8]\cdot MV]_0 + k_d$ (eq S12 in the Supporting Information). A diffusion-controlled reaction rate of CB[8]·MV with G2-PEG would be on the order of $k_{diff} \approx 10^9$–10^{10} M^{-1} s^{-1}, as estimated from the diffusion coefficients of CB[8]·MV ($D_{CB[8]\cdot MV} = 10^{-9}$ m^2 s^{-1})[30] and G2-PEG ($D_{2Np\text{-}PEG} = 10^{-10}$ m^2 s^{-1}),[44] which were reported previously.[45] The actual association rates for the ternary complex formation, $k_a \geq 10^7$ M^{-1} s^{-1}, were found to be 2–3 orders of magnitude lower than the theoretical maximum. Nevertheless, these values are much higher than most of the rather slow association rate constants observed for other high-affinity host–guest systems or metal–ligand bonded structures[12,46,47] and are similar to those reported for cyclodextrin binary complexes.[2] Interestingly, k_a of the ternary complex formation appeared to be largely insensitive to the structure and electronic properties of the second guest (Table 1). Conversely, the dissociation rate constants (k_d) of the ternary complexes were vastly different and were directly linked to the large differences seen in the thermodynamic $K_{eq}(2)$ values (Table 1); i.e., dissociation of the energetically more stable ternary complexes proceeds with a slower rate.

Activation Energies for CB[8] Ternary Complex Formation. Stopped-flow experiments at different temperatures were carried out to estimate the Arrhenius activation energy (Ea) of the ternary complex formation (Figure 2c,d, Table S2). The small magnitude of the Arrhenius activation energy for the associative process ($Ea_a \leq 10RT$) for all G2-PEGs for which values could be obtained is in agreement with the high association rates of the second-guest-binding event and similar to the Ea for the self-diffusion of water.[48] These observations further demonstrate that shape distortion and desolvation effects of the host and the guest are of low energetic cost. Determination of reliable Arrhenius activation energies for the dissociative process (Ea_d) was hampered in many cases by the experimental errors in k_d, in particular at higher temperatures. However, for the dissociation of the CB[8]·MV·Pyr-PEG ternary complex, $Ea_d = 128 \pm 11$ kJ/mol could be obtained with good confidence (Figure 2d, Table S2). Not surprisingly, the activation barrier for the dissociation of the CB[8]·MV·Pyr-PEG ternary complex is much larger than that for the association of the complex.

Viscosity and Pressure Sensitivity of CB[8] Complex Formation. To further probe the relationship between kinetics and thermodynamics, the ternary complex binding was perturbed by both increasing solution viscosity through the addition of dextran, a polysaccharide, as well as the hydrostatic pressure. Interestingly, increasing solution viscosity *selectively* perturbs the associative process of Pyr-PEG with CB[8]·MV,

DOI: 10.1021/jacs.7b04821
J. Am. Chem. Soc. 2017, 139, 12985–12993

resulting in lower k_a values and correspondingly higher Ea_a values, while the k_d and Ea_d values of the CB[8]·MV·Pyr-PEG ternary complex remained unchanged (Figure 3, Table S3). As

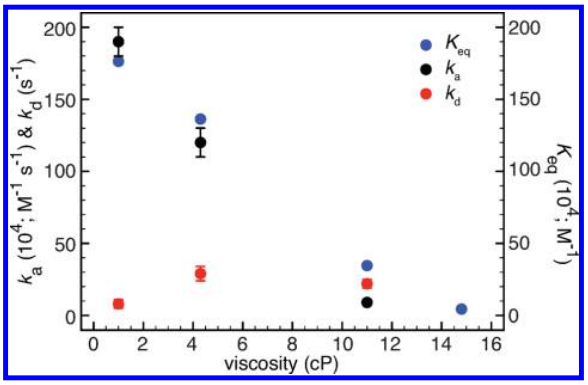

Figure 3. Determination of the viscosity dependence of CB[8] binding. Plot of k_a, k_d, and $K_{eq}(2)$ against the viscosity of the solution, which was altered through addition of dextran. The kinetic parameters were determined from stopped-flow measurements, and the thermodynamic binding constants were determined from static fluorescence binding measurements.

these measurements were made using a rapid-mixing (stopped-flow) device, we were able to increase the viscosity by approximately 10-fold (from 1 to 11 cP) before mixing artifacts compromised further measurements. Static fluorescence measurements then were performed to characterize the viscosity dependence of $K_{eq}(2)$, which was observed to decrease with increasing solution viscosity (up to 14.3 cP). The lower binding affinities observed at higher viscosities were found to be directly correlated with the slower kinetics of the associative process (k_a).

Static fluorescence and stopped-flow spectrophotometry measurements were then performed at different pressures in order to determine standard molar volume changes ($\Delta V°$) and activation volumes for the associative ($\Delta V_a^{‡}$) and dissociative ($\Delta V_d^{‡}$) processes (Figures 4 and S6). To confidently characterize kinetic parameters for the ternary complex formation using a high-pressure stopped-flow apparatus (which has a relatively long mixing dead-time of approximately 10 ms), it was necessary to slow the rate of reaction via conjugation of the MV moiety to a PEG chain of equivalent molecular weight to the G2-PEG materials, yielding MV-PEG (see Supporting Information). The binding kinetics of three different second-guests, including Pyr-PEG, DBF-PEG, and 2Np-PEG, were investigated and, in a similar manner to the alteration of solution viscosity, pressure was found to *selectively* perturb the associative process, leading to increased k_a values at higher pressures, while leaving the dissociative process unchanged (Table 2). This selective perturbation resulted in an increase in the equilibrium constant, which corroborated independent observations made in static fluorescence measurements. Interestingly, the activation volume of the associative process ($\Delta V_a^{‡}$; a measure of the degree of change of k_a with pressure) and the standard molar volume change ($\Delta V°$; a measure of the change of $K_{eq}(2)$ with pressure) were highly second-guest sensitive. Increasing the hydrophobicity of the second guest (Pyr ≫ 2Np ≫ DBF) led to a commensurate increase in both $\Delta V_a^{‡}$ and $\Delta V°$ values. These observations were further supported by characterizing the $\Delta V°$ in static measurements for three other second guests, including Flu-PEG, 1 Np-PEG, and 6-methyl-2-(4-aminophenyl)benzothiazole-PEG (BTP-PEG). The thermodynamic binding for more hydrophilic guests (i.e., those with heteroatoms; e.g., DBF and BTP) exhibit much lower pressure dependence than hydrophobic guests (e.g., Pyr and Flu), as demonstrated in Table 2.

To investigate the implications of the positive pressure dependence of the CB[8] ternary complex, we performed variable pressure steady-shear rheological measurements with supramolecular hydrogels formed with CB[8] ternary complex cross-linking of multivalent polymer chains (Figure 5a). Hydrogels were prepared according to literature protocols[8,37] using MV-functional poly(vinyl alcohol) (PVA-MV) and Np-functional polydimethylacrylamide (PDMAm-Np) polymers. The impact of pressure over the rheological properties of viscoelastic fluids is a critical aspect in many industrial processes. In hydraulic fracturing, for example, gels comprising guar gum or poly(vinyl alcohol) cross-linked with boron compounds (e.g., borax) carrying sand, or more generally "proppant", are pumped at high pressure into the hydrocarbon bearing zone of a subterranean rock formation. These gels serve to propagate and maintain appropriate fracture width while avoiding proppant sedimentation before reaching the fractured rock. The cross-links in a typical borate-cross-linked guar gel comprise bis(diol)−borate complexes that are transient in nature,[49] similar to CB[8] cross-linked gels.[8,37] This feature confers several desirable characteristics to the gel, including

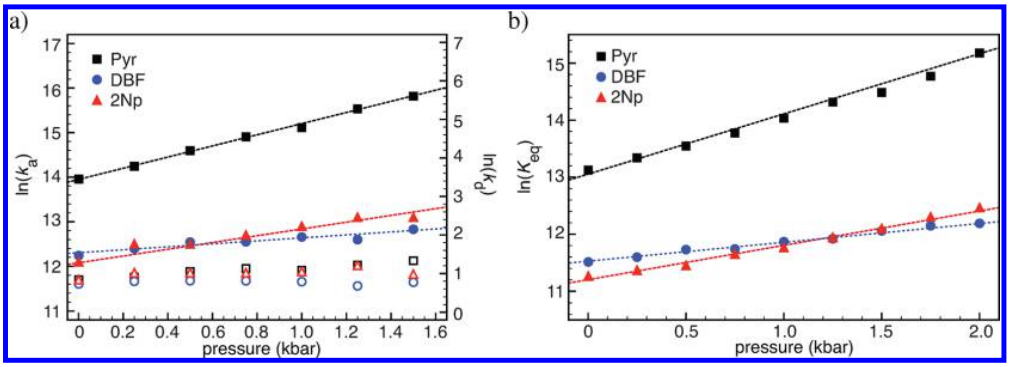

Figure 4. Determination of the pressure dependence of CB[8] binding. (a) Plot of k_a (closed symbols) and k_d (open symbols) against pressure determined with stopped-flow measurements. (b) Plot of the thermodynamic equilibrium constant against pressure determined from static fluorescence measurements.

DOI: 10.1021/jacs.7b04821
J. Am. Chem. Soc. 2017, 139, 12985−12993

Table 2. Pressure Sensitivity of CB[8] Ternary Complex Formation at 5 °C

guest	$\Delta V^{\circ a}$ (cm^3/mol)	$K_{eq}(2)^{\circ b}$ (10^4; M^{-1})	$k_a{}^c$ (10^5; M^{-1} s^{-1})	$\Delta V_a^{\ddagger}$ (cm^3/(mol·K))	$k_d{}^d$ (s^{-1})	$\Delta V_d^{\ddagger}$ (cm^3/(mol·K))
1 Np-PEG	−15.2 ± 0.6	4.0 ± 0.2				
2Np-PEG	−13.5 ± 0.7	18.1 ± 0.5	4.9 ± 0.6	15.4 ± 1.4	2.7 ± 0.3	2.8 ± 1.6
Flu-PEG	−18.6 ± 0.5	34.9 ± 0.6				
DBF-PEG	−8.6 ± 0.4	16.8 ± 0.4	3.7 ± 0.8	7.6 ± 1.2	2.2 ± 0.2	−0.4 ± 0.9
BTP-PEG	−9.2 ± 0.5	8.1 ± 0.2				
Pyr-PEG	−24.7 ± 0.8	19.5 ± 0.5	74.0 ± 1.3	28.6 ± 0.5	3.8 ± 0.2	7.1 ± 0.8

[a]Determined using static fluorescence measurements. [b]Determined using static fluorescence measurements and reported for 1500 bar. [c]Determined from k_{obs} and the $K_{eq}(2)$ according to eq S16 and reported for 1500 bar. [d]Calculated from k_a and $K_{eq}(2)$ according to $K_{eq}(2) = k_a/k_d$.

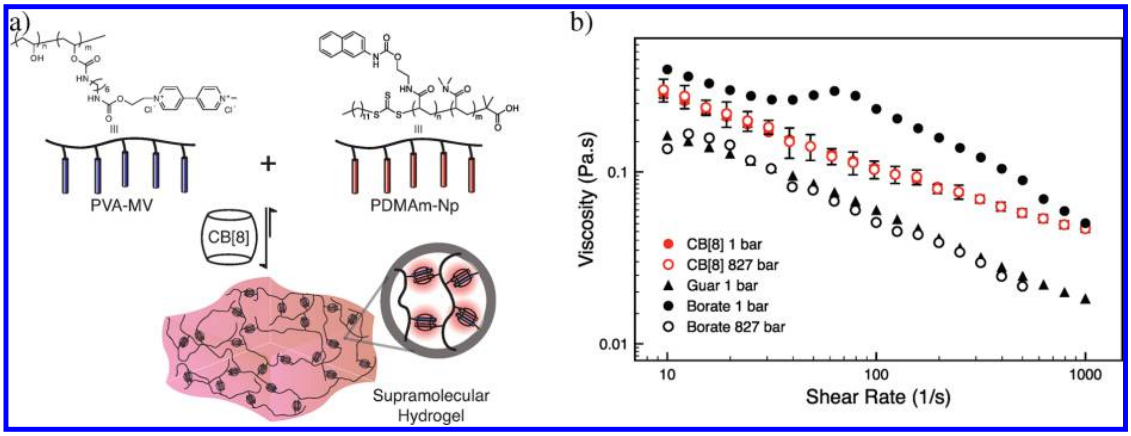

Figure 5. Characterization of the pressure dependence of CB[8]-based hydrogel rheology. (a) Schematic illustration of CB[8]-based hydrogel preparation. (b) Plot of steady-shear viscosity measurements at different pressures demonstrates that CB[8]-based hydrogel rheology (n = 3; mean ± s.d.) is unaltered by pressure (*n.b.*, the data sets for the CB[8] based gels at both 1 and 827 bar overlay one another), while traditional borate-cross-linked guar hydrogels demonstrate dramatically reduced viscosity at higher pressure on account of pressure-dependent decomplexation of the borate-diol cross-links.

tunability, shear-thinning, and shear-recovery properties; however, borate-cross-linked fluids suffer from pressure-induced thinning (Figure 5b), which has been associated with a pressure-driven dissociation of the borate ester complexes responsible for cross-linking.[50] As a consequence, an uncontrolled gel viscosity loss at high hydrostatic pressures—such as those encountered during deep water hydraulic fracturing—can have significant implications for proppant transport and fracture design. It is therefore desirable to identify dynamic cross-linking motifs which are capable of operating in aqueous media and can withstand high pressures. At ambient conditions, borate-cross-linked guar gels generally display shear-thinning behavior, with a shear-thickening regime appearing in a narrow range of intermediate shear rates (Figure 5b). The shear-thinning behavior is associated with a shear-induced decomplexation of the bis(diol)−borate cross-linking motifs, whereas the shear-thickening behavior has been related to a shear-induced increase in cross-link density and non-Gaussian chain stretching.[51] When hydrostatic pressure increases to ca. 830 bar, the viscosity of the system significantly drops at all shear rates, matching that of guar solutions in the absence of borax (Figure 5b). In contrast, the shear-dependent viscosity of hydrogels prepared through CB[8]-based cross-linking of PVA-MV and PDMAm-Np, which also exhibit shear-thinning behavior, remains unchanged as the pressure increased from ambient to ca. 830 bar (Figure 5b). While the K_{eq} increasing substantially over this range of pressure, the proportion of second guest bound (i.e., the degree of cross-linking) at the concentrations within these hydrogels increases by only 1%, corroborating our observations of relative pressure insensitivity of the hydrogel rheology.

DISCUSSION

In previous studies demonstrating the use of the CB[8] ternary system for dynamically cross-linking of multivalent polymer chains,[8,35,36] the associative rate constant of the 2Np-based ternary complex was determined to be $k_a \approx 10^6$−10^7 M^{-1} s^{-1}, depending on the polymer to which the guest was appended. This value is in good agreement with the k_a values reported herein for CB[8]·MV and the suite of G2-PEGs investigated, despite having been determined for multivalent side-chain functional polymers. Since both thermodynamic strength and the rate of formation of a non-covalent interaction are key for the dynamic behavior of diverse supramolecular materials, we seek to understand the influence of the guest structure on both the kinetic rates and equilibrium binding constants. Most strikingly, we find that the associative rates for the ternary complex formation appear to be largely independent of the structure of the guest moiety, despite the large differences in thermodynamic binding strength. Therefore, neither the distortion of the CB[8] host,[52] desolvation of the guest,[22] nor the appearance of non-covalent interactions between the host and the guest seems to be rate-limiting, even though these effects do have a clear influence on the equilibrium binding constants.[53] The experimentally determined k_a and Ea_a values, however, do not show systematic differences. This observation suggests, for example, that physical distortions of the CB[8] host can be fast at ambient temperature (see Supporting

DOI: 10.1021/jacs.7b04821
J. Am. Chem. Soc. 2017, 139, 12985−12993

Information for details) and are thus not the main determinant of the differences in the thermodynamic binding constants observed. Furthermore, from the similarity of the k_a values, it is also unlikely that the desolvation of the second-guest moiety is rate limiting, even though previous reports have demonstrated that the *thermodynamic* binding strength of the ternary complex formation is largely dependent on the solvation energies and size of the second guests.[22,23] On the other hand, the insensitivity of the k_a values to the structure of the second guest can be understood if the desolvation of the host cavity is the rate-limiting step, corroborating recent reports,[16,54] highlighting that the association process for the ternary complex formation is host-controlled. In contrast, the highly guest-sensitive dissociation rates, leading to the observed variation in overall thermodynamic binding equilibria between guests, indicates that the dissociative process is guest-controlled and is perhaps closely related to the resolvation of the guest moiety upon dissociation of the CB[8]·MV·G2 complex.

From these observations it is apparent that the associative process is "host-controlled" while the dissociative process is "guest-controlled". As differing molecular features are responsible for these two processes, it was hypothesized that a decoupling of the rate-determining factors for the associative and dissociative processes exists that could be exploited by either increasing the solution viscosity or the hydrostatic pressure of the system. Indeed, both of these external stimuli were observed to selectively perturb the associative process (Figure 6). In the case of increased solution viscosity, an overall

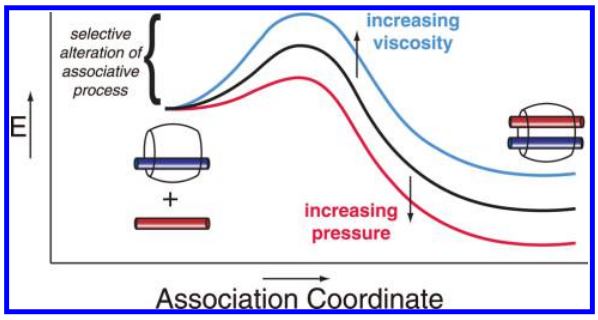

Figure 6. Schematic illustration of the reaction coordinate diagram of cucurbit[8]uril ternary complex formation. CB[8]-mediated ternary complex formation exhibits a unique combination of a high equilibrium binding strength in water *and* a high associative rate, which results in the almost instantaneous formation of strong non-covalent bonds. The rate-limiting transition state for the second-guest-binding event is located "early" on the reaction coordinate and is structurally similar for all second guests. The associative process can be *selectively* perturbed with external stimuli including solution viscosity (slower association and lower K_{eq}) or pressure (faster association and higher K_{eq}). This phenomenon affords user-defined control over the thermodynamics and kinetics of CB[8]-based ternary complex formation.

decrease in the thermodynamic binding equilibria is observed on account of the corresponding decrease in associative kinetic rate constants. In contrast, increased pressure leads to an increase in the associative rate constant, thereby leading to increased equilibrium binding constants at higher pressures. Increasing the hydrophobicity of the second guest leads to greater pressure dependence, an observation that superficially contradicted the observations made previously where the associative process was controlled primarily by the CB[8] host. It is, however, possible to develop a more nuanced understanding of the binding mechanism from these observations. At high pressures in aqueous solutions, diffusion rates and solvation of the host are expected to increase, while the unfavorable self-aggregation of the hydrophobic second guests is expected to decrease. Therefore, the increased pressure is expected to exacerbate the highly unfavorable solvation of the CB[8] cavity in the CB[8]·MV binary complex, allowing for the possibility of large enthalpic gains upon complexation with the second guest and desolvation of the host cavity.[16] However, as the solvation of the second guest is also expected to increase at high pressure, those guests prone to self-aggregation (i.e., more hydrophobic guests) at the high concentrations used for the high-pressure stopped-flow experiments (0.5 mM) will have greater capacity to form the CB[8]·MV·G2-PEG ternary complex at higher pressure. This phenomenon gives rise to the second-guest structure dependence observed in the associative process with increasing pressure across all six second guests investigated. Further, the commensurate increase in thermodynamic binding equilibria carry important implications in the application of the CB[8] ternary complex for the formation of hydrogels, as these gels show pressure-insensitive rheological properties. The impact of pressure over the rheological properties of viscoelastic fluids is a critical aspect in many industrial processes, including hydraulic fracturing, where dynamic cross-linking motifs which are capable of operating in aqueous media and can withstand high pressures have been highly sought after.

It is worth noting that the kinetic parameters for the ternary complex formation, i.e., similar k_a values but second-guest-sensitive k_d values, small Ea_a values but much larger Ea_d values, are in good agreement with the prediction for the Hammond postulate[55] for exergonic reactions. Specifically, the rate-limiting transition state for the second-guest-binding event is located "early" on the reaction coordinate and is structurally similar for all second guests (Figure 6). This interpretation is consistent with catastrophe theory, which suggests that Hammond's postulate should work best in the limit of small activation barriers.[56] CB[8]-mediated ternary complex formation, therefore, exhibits a unique combination of a high equilibrium binding strength in water and a high associative rate, which results in the almost instantaneous formation of strong non-covalent bonds. Neither the widely employed cyclodextrin-based complexes nor metal–ligand bonds combine both of these important features, which results in marked shortcomings in the materials strength or self-healing properties of materials based on these supramolecular tools, respectively. Moreover, the ability to selectively perturb the associative process with external stimuli affords user-defined control over the thermodynamics and kinetics of CB[8]-based ternary complex formation.

■ CONCLUSION

In summary, inclusion of electron-rich aromatic guests to form 1:1:1 ternary complexes with CB[8]·MV proceeds with a very high rate constant ($k_a \geq 10^7$ M^{-1} s^{-1}) and low activation energy, regardless of the nature of the second guest. The dissociative rate constant k_d values are 4–6 orders of magnitude lower than the corresponding k_a values and show a strong dependence on the second-guest structure, paralleling the trends in the thermodynamic binding selectivities. All of the available experimental data are in agreement with the predictions of Hammond's postulate for exergonic reactions

DOI: 10.1021/jacs.7b04821
J. Am. Chem. Soc. 2017, 139, 12985–12993

and suggest that for each of the second guests an early, structurally similar rate-limiting transition state occurs during the ternary complex formation. In the limit of small activation barriers and path lengths, catastrophe theory provides a basis for Hammond's postulate,[56] where the transition state resembles the higher energy minimum in CB[8]·MV with a dissociated second guest. Differing molecular features direct the associative and dissociative processes, mimicking naturally occurring reactions and giving rise to independent control over the kinetic processes within the CB[8] ternary binding equilibrium. A high degree of flexibility, therefore, exists in the design of host−guest systems with tunable dynamics and thermodynamics for tailor-made applications across a broad range of fields. Furthermore, on account of the fast (dis)-assembly rates for CB[8]-mediated ternary complexes, application of the ternary binding motif in switchable/self-healing materials or sensing assays could provide significant advantages in the stimuli-response times over other high-affinity supramolecular systems characterized by kinetically slow or inert bonds.

EXPERIMENTAL SECTION

Materials. ^{1}H NMR spectra were recorded on an Avance 500 BB-ATM (500 MHz) spectrometer in deuterium oxide. UV/visible spectra were recorded on a Varian Cary 4000 UV−vis spectrophotometer with 0.5 nm resolution in water. G2-PEG and MV-PEG polymers,[43] cucurbit[8]uril,[14] PDMAm-Np,[8] and PVA-MV polymers[37] were prepared according to literature procedures. Guar−borate gels were prepared according to literature procedures,[50] whereby guar (M_v = 3 MDa) and sodium tetraborate decahydrate (borax) were dissolved in water at 4000 and 60 ppm respectively, and the pH was adjusted to 8.5 by addition of a sodium hydroxide to form a gel, which was allowed to stand for 24 h before rheological measurements were performed. All other materials were purchased from Aldrich and used as received.

Computational Methods. Ab initio/DFT calculations were performed using the Spartan08 software package from Wavefunction. The main intention was to estimate the maximum distortion needed for the host CB[8] upon ternary complex formation. Pyr-$NHCOOCH_3$ and Ant-$NHCOOCH_3$ were taken as models for the second-guest moieties in G2-PEG and starting geometries were built using standard bond lengths and bond angles and subsequently geometry optimized (HF/3-21G). The starting geometry of MV was built using standard bond lengths and bond angles and subsequently geometry optimized (HF/3-21G). The starting geometries for the CB[8] were taken from crystal-structure (REDMET). Starting geometries of ternary complexes CB[8]·MV·Pyr-$NHCOOCH_3$ and CB[8]·MV·Ant-$NHCOOCH_3$ were obtained by manual insertion of the guests into the cavity of CB[8] and subsequent geometry optimization (HF/3-21G). In particular for the CB[8]·MV·Pyr-$NHCOOCH_3$ ternary complex, the host CB[8] displayed an elliptical distortion, compared to the circular structure of the CB[8] host alone in the absence of guests. In order to estimate the strain energy of the host upon distortion, the guests were removed, and the elliptical CB[8] was further geometry optimized (DFT/B3LYP/6-31G*) while the carbonyl−C−carbonyl−C distances were restrained along the elliptic axes. A circular structure starting from a CB[8] crystal structure (REDMET) was geometry optimized (DFT/B3LYP/6-31G*) as the energetic reference. After the restraints were removed, SP energies of both the elliptical and circular CB[8] structures were computed with DFT/B3LYP/6-31G*. The difference of ca. 5 kJ/mol between the elliptical and circular CB[8] serves as an estimate of the strain energy required for elliptical distortion of CB[8].

Determination of Solution Binding Constants by Fluorescence Titrations Experiments. Fluorescence spectra were recorded on a Cary Eclipse spectrofluorometer at 25 °C in a Spectrosil quartz cuvette (170−2700 nm spectral range, 3.5 mL volume, 10 mm path-length) equipped with a magnetic stir bar. To a solution of G2-PEG (2 μM, 1.5 mL) in deionized water (Millipore, 18.2 MΩ·cm) was titrated a solution of CB[8]·MV (100 μM) in the stock, and the fluorescence spectra were recorded after 30 s of mixing time. The data were analyzed with a 1:1 binding model taken from the literature[57] utilizing the Origin 7.0 software package. In all cases, a strong quenching of the fluorescence was observed upon addition of CB[8]·MV to a G2-PEG solution (Figure S2) whereas the quenching is much weaker in the absence of the CB[8] host. High-viscosity measurements were performed in the same manner yet with aqueous solutions of dextran (MW = 40 kDa). For high-pressure fluorescence experiments up to 2000 bar, samples were loaded into a round-bottom quartz cuvette (custom-designed for high-pressure studies) ensuring no air bubbles. This was then installed into a high-pressure fluorescence cell (ISS Inc., Champaign, IL) and immersed in water. The high-pressure cell was installed into the fluorometer, an FLS-920 fitted with a custom-built mounting plate (Edinburgh Instruments, Edinburgh, UK).

Determination of Solution Binding Constants by ITC. Titration experiments were carried out on a VIP-ITC from Microcal Inc. at 25 °C in deionized water (Millipore, 18.2 MΩ·cm). The binding equilibria were studied using a cellular CB[8]·MV concentration of 0.1 mM to which a 1.2 mM solution of G2-PEG in water was titrated. Typically 20−30 consecutive injections of 10 μL each were used. Not surprisingly, amphiphilic G2-PEG aggregated (likely in the form of micelles) in aqueous solutions in the mM concentration range, and consequently deaggregation heats had to be accounted for upon ternary complex formation. Therefore, heats of dilution were determined by titration of the G2-PEG solution into water and subtracted from the binding isotherms prior to curve fitting. Fortunately, such deaggregation heats, as determined by titration of the G2-PEG solution into water, were small in all cases except for Ant-PEG and could readily be taken into account. The data were analyzed utilizing the ITC "one set of sides" fitting function (Origin 7.0 software package) after the first data point was removed from the data set. Such obtained thermodynamic parameters confirmed that the ternary complex formation is enthalpically driven but entropically unfavorable, closely resembling previous observations for small-molecule ternary complexes.[22−25,58]

Determination of Rate Constants by Stopped-Flow Experiments. Stopped-flow photophysical measurements at ambient pressure were performed using an Applied Physics stopped-flow instrument with a 320 nm filter. The data were collected using Pro Data SX software for 10 repeats of each experiment and analyzed using Origin 7.0 software. High-pressure kinetic experiments up to 1500 bar were performed using a Hi-Tech Scientific HPSF-56 high-pressure stopped-flow spectrophotometer (TgK Scientific, Bradford on Avon, UK). The accompanying Kinetic Studio software (TgK Scientific) was used to analyze the data. Fittings for the ternary complex formation experiments performed with each of the functional polymers were made to a single-exponential decay, and averages and standard deviations are reported.

Experimental Protocols for Second-Guest Binding. For kinetics experiments a 2 μM solution of G2-PEG polymer was injected into the reaction cell 1:1 v/v with solutions of CB[8]·MV at 10, 20, 40, 70, and 100 μM. The experiments were performed through a range of temperatures including 5, 7.5, 10, 12.5, 15, 17.5, 20, 22.5, and 25 °C. In several cases the observed rate constants, k_{obs}, were too fast to be measured appropriately at higher temperatures, and a range between 5 and 15 °C was used. The observed rate constants, k_{obs}, were recovered by fitting the kinetic traces for each of 10 experiments recorded at each CB[8]·MV concentration to a single exponential decay according to $I = I_0 + I_\infty e^{-k_{obs}t}$ (I_0 and I_∞ are respectively the intensities at time zero and the total amplitude for the kinetics). The average and standard derivation of k_{obs} were calculated and used for subsequent fittings with the Origin 7.0 software package. By plotting k_{obs} against the concentration of CB[8]·MV present in the cell, both the association and dissociation rate constants (k_a and k_d, respectively) for the complexation of CB[8]·MV with the second-guest moiety could be obtained according to equation S12. The viscosity dependence of these parameters was determined by performing the

DOI: 10.1021/jacs.7b04821
J. Am. Chem. Soc. 2017, 139, 12985−12993

above-mentioned measurements in solutions of dextran (MW 40 kDa).

Experimental Protocols for High-Pressure Rheometry. Variable-pressure steady-shear measurements were performed on an Anton Paar MCR302 rheometer equipped with a C-ETD 300/PR 1000 high-pressure cell. This equipment is designed for pressures to 1000 bar and temperatures to 290 °C and employs and narrow-gap Couette geometry. The bob has a diameter of 29.5 mm and a height of 40.0 mm, with the cup having a diameter of 30.0 mm. The cell of the rheometer is coupled to a 65D ISCO pump, which enables the loading of fluids into the rheometer cell prior to analysis while maintaining a constant pressure during measurements.

■ ASSOCIATED CONTENT

Supporting Information

The Supporting Information is available free of charge on the ACS Publications website at DOI: 10.1021/jacs.7b04821.

^{1}H NMR, GPC, ITC, and stopped-flow measurements (PDF)

■ AUTHOR INFORMATION

Corresponding Authors

*eappel@stanford.edu
*frank.biedermann@kit.edu
*oas23@cam.ac.uk

ORCID

Eric A. Appel: 0000-0002-2301-7126
Sam Hay: 0000-0003-3274-0938
Oren A. Scherman: 0000-0001-8032-7166

Notes

The authors declare no competing financial interest.

■ ACKNOWLEDGMENTS

E.A.A. thanks Schlumberger for financial support, and F.B. thanks the German Academic Exchange Service (DAAD). This work was supported in part by the Walters-Kundert foundation, an ERC Starting Investigator grant (ASPiRe), and the Biotechnology and Biological Sciences Research Council (BB/H021523/1).

■ REFERENCES

(1) Dsouza, R. N.; Hennig, A.; Nau, W. M. *Chem. - Eur. J.* **2012**, *18*, 3444−3459.
(2) Tang, H.; Fuentealba, D.; Ko, Y. H.; Selvapalam, N.; Kim, K.; Bohne, C. *J. Am. Chem. Soc.* **2011**, *133*, 20623−20633.
(3) Appel, E. A.; del Barrio, J.; Loh, X. J.; Scherman, O. A. *Chem. Soc. Rev.* **2012**, *41*, 6195−6214.
(4) Burnworth, M.; Tang, L.; Kumpfer, J. R.; Duncan, A. J.; Beyer, F. L.; Fiore, G. L.; Rowan, S. J.; Weder, C. *Nature* **2011**, *472*, 334−337.
(5) Fox, J.; Wie, J. J.; Greenland, B. W.; Burattini, S.; Hayes, W.; Colquhoun, H. M.; Mackay, M. E.; Rowan, S. J. *J. Am. Chem. Soc.* **2012**, *134*, 5362−5368.
(6) Yount, W. C.; Loveless, D. M.; Craig, S. L. *J. Am. Chem. Soc.* **2005**, *127*, 14488−14496.
(7) Yount, W. C.; Loveless, D. M.; Craig, S. L. *Angew. Chem.* **2005**, *117*, 2806−2808.
(8) Appel, E. A.; Forster, R. A.; Koutsioubas, A.; Toprakcioglu, C.; Scherman, O. A. *Angew. Chem., Int. Ed.* **2014**, *53*, 10038−10043.
(9) Grindy, S. C.; Learsch, R.; Mozhdehi, D.; Cheng, J.; Barrett, D. G.; Guan, Z.; Messersmith, P. B.; Holten-Andersen, N. *Nat. Mater.* **2015**, *14*, 1210−1216.
(10) Gaspari, R.; Rechlin, C.; Heine, A.; Bottegoni, G.; Rocchia, W.; Schwarz, D.; Bomke, J.; Gerber, H.-D.; Klebe, G.; Cavalli, A. *J. Med. Chem.* **2016**, *59*, 4245−4256.
(11) Klebe, G. *ChemMedChem* **2015**, *10*, 229−231.
(12) Lagona, J.; Mukhopadhyay, P.; Chakrabarti, S.; Isaacs, L. *Angew. Chem., Int. Ed.* **2005**, *44*, 4844−4870.
(13) Masson, E.; Ling, X. X.; Joseph, R.; Kyeremeh-Mensah, L.; Lu, X. Y. *RSC Adv.* **2012**, *2*, 1213−1247.
(14) Kim, J.; Jung, I. S.; Kim, S. Y.; Lee, E.; Kang, J. K.; Sakamoto, S.; Yamaguchi, K.; Kim, K. *J. Am. Chem. Soc.* **2000**, *122*, 540−541.
(15) Day, A. I.; Blanch, R. J.; Arnold, A. P.; Lorenzo, S.; Lewis, G. R.; Dance, I. *Angew. Chem., Int. Ed.* **2002**, *41*, 275−277.
(16) Biedermann, F.; Uzunova, V. D.; Scherman, O. A.; Nau, W. M.; De Simone, A. *J. Am. Chem. Soc.* **2012**, *134*, 15318−15323.
(17) Nau, W. M.; Florea, M.; Assaf, K. I. *Isr. J. Chem.* **2011**, *51*, 559−577.
(18) Kim, H.-J.; Heo, J.; Jeon, W. S.; Lee, E.; Kim, J.; Sakamoto, S.; Yamaguchi, K.; Kim, K. *Angew. Chem., Int. Ed.* **2001**, *40*, 1526−1529.
(19) Lee, J. W.; Samal, S.; Selvapalam, N.; Kim, H. J.; Kim, K. *Acc. Chem. Res.* **2003**, *36*, 621−630.
(20) Ko, Y. H.; Kim, K.; Kang, J. K.; Chun, H.; Lee, J. W.; Sakamoto, S.; Yamaguchi, K.; Fettinger, J. C.; Kim, K. *J. Am. Chem. Soc.* **2004**, *126*, 1932−1933.
(21) Lee, J. W.; Kim, K.; Choi, S.; Ko, Y. H.; Sakamoto, S.; Yamaguchi, K.; Kim, K. *Chem. Commun.* **2002**, 2692−2693.
(22) Rauwald, U.; Biedermann, F.; Deroo, S.; Robinson, C. V.; Scherman, O. A. *J. Phys. Chem. B* **2010**, *114*, 8606−8615.
(23) Biedermann, F.; Scherman, O. A. *J. Phys. Chem. B* **2012**, *116*, 2842−2849.
(24) Bush, M. E.; Bouley, N. D.; Urbach, A. R. *J. Am. Chem. Soc.* **2005**, *127*, 14511−14517.
(25) Heitmann, L. M.; Taylor, A. B.; Hart, P. J.; Urbach, A. R. *J. Am. Chem. Soc.* **2006**, *128*, 12574−12581.
(26) Tian, F.; Cziferszky, M.; Jiao, D.; Wahlström, K.; Geng, J.; Scherman, O. A. *Langmuir* **2011**, *27*, 1387−1390.
(27) Tian, F.; Cheng, N.; Nouvel, N.; Geng, J.; Scherman, O. A. *Langmuir* **2010**, *26*, 5323−5328.
(28) An, Q.; Brinkmann, J.; Huskens, J.; Krabbenborg, S.; de Boer, J.; Jonkheijm, P. *Angew. Chem., Int. Ed.* **2012**, *51*, 12233−12237.
(29) Young, J. F.; Nguyen, H. D.; Yang, L.; Huskens, J.; Jonkheijm, P.; Brunsveld, L. *ChemBioChem* **2010**, *11*, 180−183.
(30) Biedermann, F.; Rauwald, U.; Zayed, J. M.; Scherman, O. A. *Chemical Science* **2011**, *2*, 279−286.
(31) Nguyen, H. D.; Dang, D. T.; van Dongen, J. L. J.; Brunsveld, L. *Angew. Chem., Int. Ed.* **2010**, *49*, 895−898.
(32) Dang, D. T.; Schill, J.; Brunsveld, L. *Chem. Sci.* **2012**, *3*, 2679−2684.
(33) Zhang, J.; Coulston, R. J.; Jones, S. T.; Geng, J.; Scherman, O. A.; Abell, C. *Science* **2012**, *335*, 690−694.
(34) Coulston, R. J.; Jones, S. T.; Lee, T.-C.; Appel, E. A.; Scherman, O. A. *Chem. Commun.* **2011**, *47*, 164−166.
(35) Appel, E. A.; Dyson, J.; del Barrio, J.; Walsh, Z.; Scherman, O. A. *Angew. Chem., Int. Ed.* **2012**, *51*, 4185−4189.
(36) Appel, E. A.; Biedermann, F.; Rauwald, U.; Jones, S. T.; Zayed, J. M.; Scherman, O. A. *J. Am. Chem. Soc.* **2010**, *132*, 14251−14260.
(37) Appel, E. A.; Loh, X. J.; Jones, S. T.; Biedermann, F.; Dreiss, C. A.; Scherman, O. A. *J. Am. Chem. Soc.* **2012**, *134*, 11767−73.
(38) Appel, E. A.; Loh, X. J.; Jones, S. T.; Dreiss, C. A.; Scherman, O. A. *Biomaterials* **2012**, *33*, 4646−4652.
(39) Rowland, M. J.; Appel, E. A.; Coulston, R. J.; Scherman, O. A. *J. Mater. Chem. B* **2013**, *1*, 2904−2910.
(40) Appel, E. A.; Forster, R. A.; Rowland, M. J.; Scherman, O. A. *Biomaterials* **2014**, *35*, 9897−9903.
(41) Biedermann, F.; Rauwald, U.; Cziferszky, M.; Williams, K. A.; Gann, L. D.; Guo, B. Y.; Urbach, A. R.; Bielawski, C. W.; Scherman, O. A. *Chem. - Eur. J.* **2010**, *16*, 13716−13722.
(42) A lower limit for the kinetic rate constants of a second-guest binding to CB[8]·MV can be derived from the observation that ternary complex formation is fast on the NMR time scale.
(43) Biedermann, F.; Appel, E. A.; del Barrio, J.; Gruendling, T.; Barner-Kowollik, C.; Scherman, O. A. *Macromolecules* **2011**, *44*, 4828−4835.

DOI: 10.1021/jacs.7b04821
J. Am. Chem. Soc. 2017, 139, 12985−12993

(44) Zayed, J. M.; Biedermann, F.; Rauwald, U.; Scherman, O. A. *Polym. Chem.* **2010**, *1*, 1434−1436.
(45) $k_{diff} = 4\pi(D_{CB[8]\cdot MV} + D_{2Np\text{-}PEG})(r_{CB[8]\cdot MV} + r_{second\text{-}guest})N_A/10^{-3}$ m^3 with the approximated radii $r_{CB[8]\cdot MV} = 10^{-9}$ m and $r_{second\text{-}guest} = 5^{-10}$ m and Avogadro's number N_A.
(46) Mukhopadhyay, P.; Zavalij, P. Y.; Isaacs, L. *J. Am. Chem. Soc.* **2006**, *128*, 14093−14102.
(47) Marquez, C.; Hudgins, R. R.; Nau, W. M. *J. Am. Chem. Soc.* **2004**, *126*, 5806−5816.
(48) Talekar, S. V. *Int. J. Quantum Chem.* **1977**, *12*, 459−469.
(49) Kesavan, S.; Prud'homme, R. K. *Macromolecules* **1992**, *25*, 2026−2032.
(50) Parris, M. D.; MacKay, B. A.; Rathke, J. W.; Klingler, R. J.; Gerald, R. E. *Macromolecules* **2008**, *41*, 8181−8186.
(51) Hu, Y. T. *J. Rheol.* **2014**, *58*, 1789−1807.
(52) DFT calculations (B3LYP/6-31G*) yielded a higher strain energy by 5 kJ/mol when CB[8] was elliptically distorted where such a distortion is required to bind the larger pyrene unit as opposed to the more narrow and shallow naphthalene/anthracene moieties.
(53) Biedermann, F.; Schneider, H. J. *Chem. Rev.* **2016**, *116*, 5216−5300.
(54) Biedermann, F.; Nau, W. M.; Schneider, H.-J. *Angew. Chem., Int. Ed.* **2014**, *53*, 11158−11171.
(55) Hammond, G. S. *J. Am. Chem. Soc.* **1955**, *77*, 334.
(56) Wales, D. J. *Science* **2001**, *293*, 2067−2069.
(57) Douhal, A. *Cyclodextrin Materials Photochemistry, Photophysics and Photobiology (Chemical, Physical and Biological Aspects of Confined Systems)*; Elsevier Science Ltd: Amsterdam, 2006.
(58) Biedermann, F.; Elmalem, E.; Ghosh, I.; Nau, W. M.; Scherman, O. A. *Angew. Chem., Int. Ed.* **2012**, *51*, 7739−7743.

DOI: 10.1021/jacs.7b04821
J. Am. Chem. Soc. 2017, 139, 12985−12993